Studies on Models for Tetrahydrofolic Acid. III. Hydrolytic Interconversions of the Tetrahydroquinoxaline Analogs at the Formate Level of Oxidation

S. J. Benkovic,*[1] W. P. Bullard,[2] and P. A. Benkovic

Contribution from the Department of Chemistry, The Pennsylvania State University, University Park, Pennsylvania 16802.
Received September 13, 1971

Abstract: Hydrolysis of the formamidinium salts IV–VI was studied as a function of pH and buffer concentration as a model for nonenzymic interconversion of formate-carrying tetrahydrofolic acid. Rates for the *p*-ethoxycarbonylformamidinium salt hydrolysis determined above pH 6 exhibited first-order kinetics with marked buffer catalysis by all buffers studied. Rates measured at pH ≤ 6 exhibited nonlinear kinetics due to subsequent isomerization of the initially formed N^{10}-formyl product to the more stable N^{1}-formyl compound. These data are rationalized by one kinetic scheme in which all three species arise from a common intermediate or a collection of protonically related intermediates, the step for production of the N^{1}-formyl being kinetically significant only at pH ≤ 6. Each buffer used exhibited a unique catalytic facility with respect to relative rates of formation of the two *N*-formyl products. Equilibrium constants relating the *p*-ethoxycarbonylformamidinium salt to each *N*-formyl product were determined and found to be in quantitative agreement with those of the natural cofactor. The close resemblance between the kinetic and thermodynamic dispositions of the model and folate compounds supports the validity of the model and permits comment on the biological implications.

The role of 5,6,7,8-tetrahydrofolic acid (FH_4) in the metabolism of single carbon units at the formate level of oxidation has been well established.[3] Investigations of the formate-carrying cofactor in both enzymic and nonenzymic reactions have revealed at least the cursory features of these reactions.[3] Experimental difficulties with regard to the instability of the tetrahydropyrazine ring toward oxidation have discouraged extensive investigation. In light of this, various derivatives of *N*,*N'*-diarylethylenediamines and structurally related compounds have been investigated as models for the interconversion of 5,10-methenyltetrahydrofolic acid and its *N*-formyl derivative(s).[4]

The work reported here involves a study, related to interconversion of certain formate-carrying forms of FH_4, employing a model compound which embraces two features not present in the symmetrically para-substituted *N*,*N'*-diarylethylenediamines that the authors feel to be important with respect to the reactions of FH_4 specifically, the dissymmetry arising from the ΔpK_a between the participating aniline nitrogens owing to unequal electronic effects and the geometry conferred by the fused ring system. A more complete discussion concerning the design of this model has been previously published.[5]

The compounds studied were the formamidinium salts IV–VI derived from the substituted tetrahydroquinoxalines I, II, and III. The formamidinium salt synthesized from I, the model compound, most closely resembling the natural cofactor, in terms of the aforementioned ΔpK_a, was subjected to the most extensive study of the three formamidinium salts. The macroscopic ΔpK_a for III is 5.45 compared to 6.07 for FH_4.

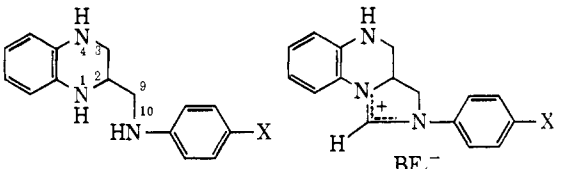

I, X = CO_2Et
II, X = Cl
III, X = CH_3

IV, X = CO_2Et
V, X = Cl
VI, X = CH_3

Results

Structure Assignments. Several lines of evidence support the structure assignments for compounds IV–VI and their related *N*-formyl derivatives. For any of the formamidinium salts, the possibility existed that bridging might occur between the exocyclic nitrogen and the N-4 of the tetrahydropyrazine ring rather than at the N-1 as desired. However, sodium borohydride reduction of the *p*-ethoxycarbonylformamidinium salt IV gave the methylene-bridged adduct involving N-1 and -10, the structure of which had been established previously.[5] Furthermore, inspection of Corey–Pauling–Koltun models indicates that the undesired bridging would, to a great extent, restrict the resonance of the N-4 with the phenyl ring which should give rise to an ultraviolet maximum characteristic of a simple *N*-arylamidine (~275 mμ) rather than the observed absorption at 365 mμ suggestive of extended conjugation.

The N^{1}-formyl and N^{10}-formyl derivatives of I were prepared by hydrolysis of IV under weakly acidic and mildly basic conditions, respectively. The structure of IV being established, it remained to distinguish between the two *N*-formyl isomers. The nmr spectra reveal, in one case, a near-singlet corresponding to the four aromatic protons of the tetrahydroquinoxaline moiety and, in the other case, a wider multiplet arising from the

(1) National Institutes of Health Career Development Awardee, Alfred P. Sloan Fellow, 1968–1970.
(2) National Science Foundation Trainee.
(3) For an extensive review see R. L. Blakley, "The Biochemistry of Folic Acid and Related Pteridines," North-Holland Publishing Co., Amsterdam, 1969.
(4) D. R. Robinson and W. P. Jencks, *J. Amer. Chem. Soc.*, 89, 7088 (1967); M. May, T. J. Bardos, F. L. Barger, M. Lansford, J. M. Ravel, G. L. Sutherland, and W. Shive, *ibid.*, 73, 3067 (1951); L. Jaenicke and E. Brode, *Justus Liebigs Ann. Chem.*, 624, 120 (1959).
(5) S. J. Benkovic, P. A. Benkovic, and D. R. Comfort, *J. Amer. Chem. Soc.*, 91, 5270 (1969).

Table I. Rate Constants for Base-Catalyzed Hydrolysis of Formamidinium Salts[a]

Compd	Base (pK_a)[b]	pH range	Runs	k_B, M^{-1} min^{-1}	$k_{B\cdot OH} \times 10^{-7}$, M^{-2} min^{-1}
IV	H_2O (−1.57)	6.20–8.50	c	0.00029 ± 0.00005	
	Succinate (5.33)	5.75–6.20	8	0.40 ± 0.07	
	Phosphate (6.75)	6.10–7.33	20	4.9 ± 1.3	5.2 ± 0.5[d]
	Tris (8.16)	7.70–8.50	20	5.4 ± 1.4	1.4 ± 0.1
	Imidazole (7.11)	6.47–7.74	13	7.7 ± 2.1	2.6 ± 0.4
	OH^- (15.7)	7.00–8.50	c	1.1 ± 0.1	
V	H_2O (−1.57)	6.10–7.33	c	0.00016 ± 0.00003	
	Phosphate (6.75)	6.10–7.33	21	2.4 ± 0.2	1.08 ± 0.08[d]
VI	H_2O (−1.57)	6.10–7.33	c	0.00011 ± 0.00001	
	Phosphate (6.75)	6.10–7.33	21	1.11 ± 0.06	0.38 ± 0.03[d]

[a] According to eq 1, $T = 25°$, $\mu = 0.2$, KCl. [b] Determined as defined in the text. [c] Spontaneous and hydroxide ion catalytic constants were determined from intercepts of k_{obsd} *vs.* $[buffer]_{total}$. The observed spontaneous rates were divided by 55.5 *M*. [d] Note that for phosphate catalysis, the term second order in base cannot be distinguished kinetically from $k'[B]$ in which $B = PO_4^{3-}$.

same protons. In light of the near-symmetry of the *o*-phenylenediamine type structure, the first spectrum is attributed to the N^{10}-formyl compound. By the same reasoning, the spectrum exhibiting the multiplet is attributed to the N^1-formyl compound in which the near-symmetry is lost due to formylation of N-1. The mass spectra, although not uniquely definitive owing to apparent cyclization during analysis, are consistent with these assignments. Both *N*-formyl compounds present a formyl proton absorption in the nmr and upon treatment with dilute acid yield quantitatively the formamidinium salt.

Structure assignments for the *p*-chloro- and *p*-methylformamidinium salts and their respective *N*-formyl derivatives were made on the basis of nmr and mass spectra by much the same reasoning. These *N*-formyl compounds can likewise be reconverted to their formamidinium salts.

Kinetics

The rates of hydrolysis of the formamidinium salts IV–VI derived from compounds I–III were measured as a function of pH and buffer concentration. The *p*-CH_3 (VI) and *p*-Cl (V) compounds were studied in phosphate buffers only, while the *p*-CO_2Et compound was studied over a wider pH range using imidazole, succinate, phosphate, and Tris buffers. Hydrolysis of all three compounds exhibited pseudo-first-order kinetics above pH 6 and followed the rate law of eq 1, in which B represents the base form of the buffer or hydroxide ion, S the formamidinium salt, and $a_{OH^-} = 10^{-14}/a_{H^+}$.

$$V\frac{1}{[S]} = k_{obsd} = k_{H_2O} + k_B[B] + k_{B\cdot OH}[B]a_{OH^-} \quad (1)$$

The values for k_{H_2O} were taken from the intercept of a plot of k_{obsd} against total buffer concentration. Values for k_B were taken as the slope of plots of k_{obsd} against [B] using rate data measured in a pH range where the term second order in base makes a relatively insignificant contribution, *i.e.* the slope is invariant with changing pH. For kinetics at pH >7 $k_{B\cdot OH}$ was calculated from eq 1 employing the appropriate values of k_{H_2O} and $k_B[B]$ for the particular buffer.

The second-order rate constant for hydroxide-catalyzed hydrolysis (k_B, B = OH^-) was taken as the slope of a plot of k' *vs.* a_{OH^-} where k' is the observed rate at zero buffer concentration (extrapolated) minus the observed spontaneous rate, k_{H_2O}.

Ultimately, these and all other parameters were subjected to adjustment by use of a nonlinear least-squares regression computer program to give the best fit to the data. The values thus obtained appear in Table I and are not corrected for product distribution (see below). The error limits assigned to the rate constants are defined as that increment by which the parameter can be altered without reducing the correlation coefficient.

Analysis of the kinetically controlled reaction products, *i.e.* where eq 1 obtains, revealed that the *p*-chloro- and *p*-methylformamidinium salts both yield the N^1-formyl product, while the *p*-CO_2Et salt yields from ~0 to ~20% N^1-formyl product depending on the nature of the buffer, the balance being the N^{10}-formyl (*cf.* Table IV). Repetitive ultraviolet scans of the reaction mixtures formed during the hydrolysis of the three formamidinium salts revealed an isosbestics point under all conditions except that of the *p*-CO_2Et compound at pH <6. Hydrolysis of this compound below pH 6 exhibited a noticeable loss of isosbestics point suggestive of some subsequent reaction of the kinetically controlled N^{10}-formyl product. Ultraviolet spectra of these reaction mixtures at times greater than 10 half-lives for hydrolysis of IV revealed a slow conversion of the N^{10}-formyl to the N^1-formyl product.

Accompanying the loss of isosbestics point is a strong deviation of the kinetics from first order. In light of the facts that (a) a kinetically significant intermediate has been demonstrated for some closely related reactions[4,6,7] and (b) both the formamidinium salt and the N^{10}-formyl compound ultimately yield the N^1-formyl product, Scheme I is proposed. The rate constants shown in Scheme I contain whatever buffer and/or lyate species is participating in that step.

Using this general scheme, the steady-state assumption for I and the technique of Rodiguin and Rodiguina,[8] six kinetic equations (eq 2–7) describing the time dependence of the concentration of the three species were derived. As Scheme I suggests, the reactions at this pH can be initiated with either the formamidinium salt or the N^{10}-formyl compound. Accordingly, eq 2–4 represent reactions begun with the N^{10}-formyl compound, while eq 5–7 represent those initiated with the formamidinium salt IV. The parameters

(6) D. R. Robinson and W. P. Jencks, *J. Amer. Chem. Soc.*, **89**, 7098 (1967).
(7) D. R. Robinson, *ibid.*, **92**, 3138 (1970).
(8) N. M. Rodiguin and E. N. Rodiguina, "Consecutive Chemical Reactions," D. van Nostrand, Princeton, N. J., 1964.

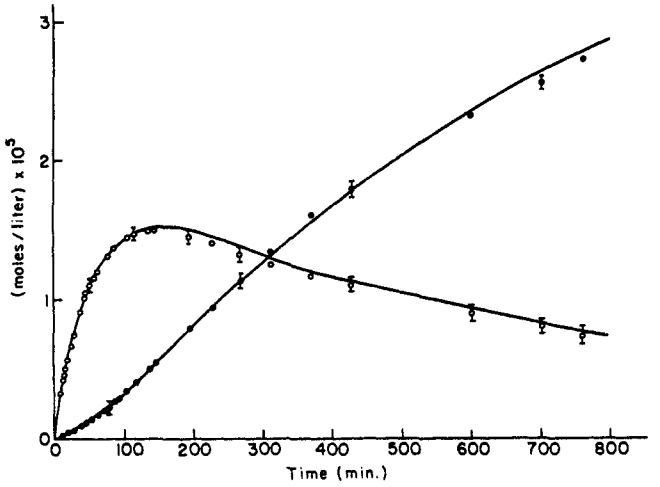

Figure 1. O, concentration of the *p*-ethoxycarbonylformamidinium salt (IV) as a function of time for the reaction initiated with N^{10}-formyl in 0.054 *M* succinate buffer, pH 5.33, $T = 25°$, $\mu = 0.2$, KCl. The curve is calculated from eq 2. ●, concentration of the *p*-ethoxycarbonyl-N^1-formyl compound as a function of time for the reaction initiated with N^{10}-formyl in 0.054 *M* succinate buffer, pH 5.33, $T = 25°$, $\mu = 0.2$, KCl. The curve is calculated from eq 3.

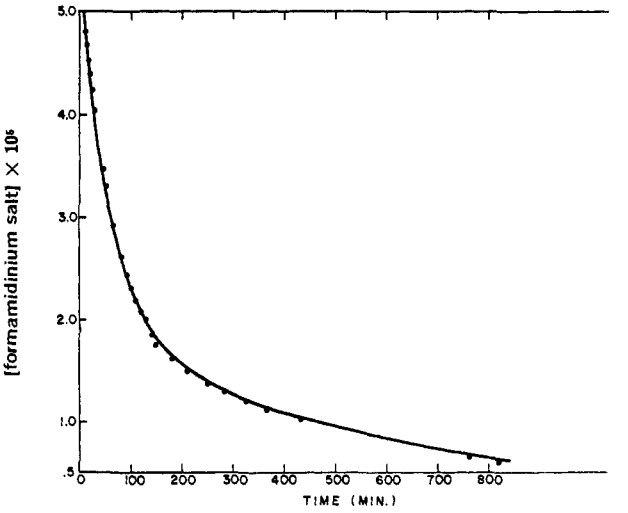

Figure 2. Concentration of the *p*-ethoxycarbonylformamidinium salt as a function of time for the reaction initiated with that compound in 0.054 *M* succinate buffer, pH 5.33, $T = 25°$, $\mu = 0.2$, KCl. The curve is calculated from eq 5.

Scheme I

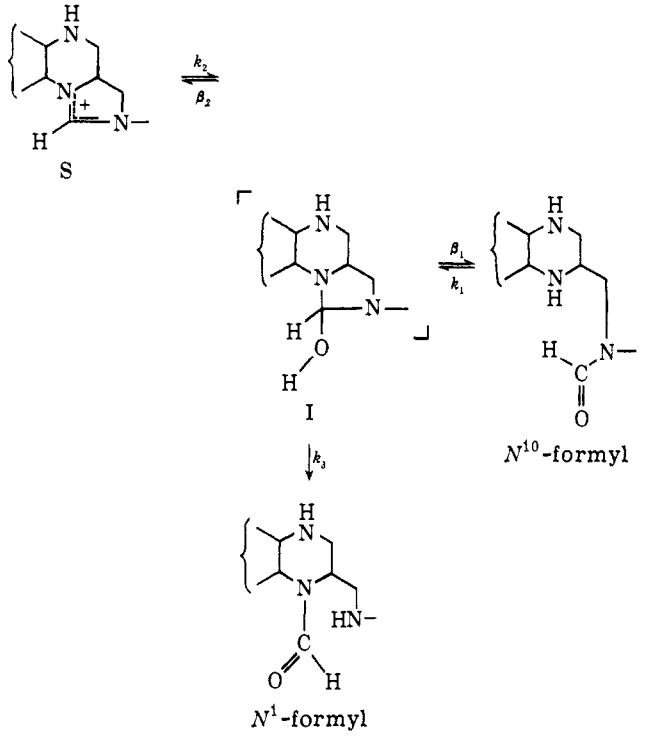

used in these equations were evaluated by computer fit and are listed in Table II.

Figures 1 and 2 illustrate the time dependence of the concentrations of the three species for the indicated reactions in 0.054 *M* succinate buffer at pH 5.33. Although eq 2 and 7 represent functions that are numerically different, the forms of the equations are similar and they will generate similar curves. That is, [N-10] = f([S]$_0$,*t*) will resemble [S] = f([N-10]$_0$,*t*) of Figure 2. The same analogy exists for eq 3 and 6 and eq 4 and 5.

Unfortunately this treatment was limited to a narrow pH range due to the reversibility of the k_3 step at lower pH and the diminution of γ_2 to less than experimental error at higher pH. Consequently, such values as the pH dependence of k_1 and k_2 of this scheme could not be determined with certainty. The parametric equations related to Scheme I are presented in the hope that they might be of general interest.

Table II. Values for Parameters of Eq 2–7 Describing [S], [N^1-Formyl], and [N^{10}-Formyl] for I[a]

No.	Parameter	Source	Value, min^{-1}
1	γ_1	All equations	0.0166 ± 0.0004
2	γ_2	All equations	0.00129 ± 0.00005
3	$\frac{\beta_2 k_1}{\beta_1 + k_3 + \beta_2}$	[S] = f([N-10]$_0$, *t*)	0.00567 ± 0.00005
4	$\frac{k_1 k_3}{\beta_1 + k_3 + \beta_2}$	[N-1] = f([N-10]$_0$, *t*)	0.00022 ± 0.00003
5	k_2	[N-1] = f([N-10]$_0$, *t*)	0.09 ± 0.01
6	$\frac{k_2(\beta_1 + k_3)}{\beta_1 + k_3 + \beta_2}$	[N-10] = f([N-10]$_0$, *t*)	0.01113 ± 0.0002
7	$\frac{\beta_1(k_3 + \beta_2)}{\beta_1 + k_3 + \beta_2}$	[S] = f([S]$_0$, *t*)	0.00643 ± 0.00005
8	$\frac{k_3 k_2}{\beta_1 + k_3 + \beta_2}$	[N-1] = f([S]$_0$, *t*)	0.0025 ± 0.0001
9	k_1	[N-1] = f([S]$_0$, *t*)	0.007 ± 0.0004
10	$\frac{\beta_1 k_2}{\beta_1 + k_3 + \beta_2}$	[N-10] = f([S]$_0$, *t*)	0.0094 ± 0.0001

[a] At time *t* in 0.054 *M* succinate, pH 5.33, $T = 25°$, $\mu = 0.2$, KCl.

$$[S] = [N\text{-}10]_0 \frac{\beta_2 k_1}{\beta_1 + k_3 + \beta_2}\left[\frac{1}{\gamma_2 - \gamma_1} e^{-\gamma_1 t} + \frac{1}{\gamma_1 - \gamma_2} e^{-\gamma_2 t}\right] \quad (2)$$

$$[N\text{-}1] = [N\text{-}10]_0 \frac{k_1 k_3}{\beta_1 + k_3 + \beta_2}\left[\frac{k_2}{\gamma_1\gamma_2} - \frac{k_2 - \gamma_1}{\gamma_1(\gamma_2 - \gamma_1)} e^{-\gamma_1 t} - \frac{k_2 - \gamma_2}{\gamma_2(\gamma_1 - \gamma_2)} e^{-\gamma_2 t}\right] \quad (3)$$

$$[N\text{-}10] = [N\text{-}10]_0 \frac{1}{\gamma_2 - \gamma_1}\left[\left(\frac{k_2(\beta_1 + k_3)}{\beta_1 + k_3 + \beta_2} - \gamma_1\right) e^{-\gamma_1 t} - \left(\frac{k_2(\beta_1 + k_3)}{\beta_1 + k_3 + \beta_2} - \gamma_2\right) e^{-\gamma_2 t}\right] \quad (4)$$

$$[S] = [S]_0 \frac{1}{\gamma_2 - \gamma_1}\left[\left(\frac{k_1(k_3 + \beta_2)}{\beta_1 + k_3 + \beta_2} - \gamma_1\right)e^{-\gamma_1 t} - \left(\frac{k_1(k_3 + \beta_2)}{\beta_1 + k_3 + \beta_2} - \gamma_2\right)e^{-\gamma_2 t}\right] \quad (5)$$

$$[N\text{-}1] = [S]_0 \frac{k_3 k_2}{\beta_1 + k_3 + \beta_2}\left[\frac{k_1}{\gamma_2\gamma_1} - \frac{k_1 - \gamma_1}{\gamma_1(\gamma_2 - \gamma_1)}e^{-\gamma_1 t} - \frac{k_1 - \gamma_2}{\gamma_2(\gamma_1 - \gamma_2)}e^{-\gamma_2 t}\right] \quad (6)$$

$$[N\text{-}10] = [S]_0 \frac{\beta_1 k_2}{\beta_1 + k_3 + \beta_2}\left[\frac{1}{\gamma_2 - \gamma_1}e^{-\gamma_1 t} + \frac{1}{\gamma_1 - \gamma_2}e^{-\gamma_2 t}\right] \quad (7)$$

Two important quantities can be calculated using the listed parameters. (1) Dividing no. 8 by no. 6 one

$$\frac{k_3 k_2}{\beta_1 + k_3 + \beta_2}\left[\frac{k_2(\beta_1 + k_3)}{\beta_1 + k_3 + \beta_2}\right]^{-1} = \frac{k_3}{\beta_1 + k_3}$$

obtains the mole fraction for partitioning of the intermediate(s) to N^1-formyl with respect to the N^1- and N^{10}-formyl products arising from the intermediate(s). (2) Dividing no. 3 by no. 10 one obtains the equilibrium value for [S]/[N^{10}-formyl] which, when divided by the a_{H^+}, gives the equilibrium constant for eq 8.

$$\frac{\beta_2 k_1}{\beta_1 + k_3 + \beta_2}\left[\frac{\beta_1 k_2}{\beta_1 + k_3 + \beta_2}\right]^{-1} = \frac{\beta_2 k_1}{\beta_1 k_2}$$

$$N^{10}\text{-formyl} + H^+ \underset{}{\overset{K_{eq}^{(N\text{-}10)}}{\rightleftharpoons}} S + H_2O$$

$$K_{eq}^{(N\text{-}10)} = [S]/[N^{10}\text{-formyl}]a_{H^+} \quad (8)$$

This constant could not be obtained by direct ultraviolet analysis since at pH values where $[S]_{eq}/[N^{10}\text{-formyl}]_{eq}$ is experimentally measurable, the k_3 step for production of N^1-formyl is significant and only a secular equilibrium obtains.

Equilibrium Constants

The equilibrium constants (Table III) relating the formamidinium salts to their respective *N*-formyl compounds were determined. In all cases, the equilibria followed eq 9 exhibiting a linear dependence on

$$K_{eq} = \frac{[S]}{[N\text{-formyl}]a_{H^+}} \quad (9)$$

a_{H^+}. The dependence of log $K_{eq}^{(N\text{-}1)}$ on the estimated pK_a of the exocyclic aniline nitrogen[9] is linear with a slope of 0.58. Note, however, that the constant for the N^{10}-formyl $\rightleftharpoons$ *p*-ethoxycarbonylformamidinium salt equilibrium is greater than that for the N-1 isomer by approximately two orders of magnitude. When $K_{eq}^{(N\text{-}10)}$ is divided by $K_{eq}^{(N\text{-}1)}$ for the *p*-CO_2Et compound, the pH-independent equilibrium for the two *N*-formyl compounds is obtained according to eq 10 with a value equal to 1.63×10^2.

$$N^{10}\text{-formyl} \rightleftharpoons N^1\text{-formyl}$$

$$K_{eq} = \frac{[N^1\text{-formyl}]}{[N^{10}\text{-formyl}]} \quad (10)$$

(9) Values for pK_a of the exocyclic nitrogens were taken as those for *p*-chloroaniline, *p*-toluidine, and *p*-carboethoxyaniline from A. Albert and E. P. Serjeant, "Ionization Constants of Acids and Bases," Wiley, New York, N. Y., 1962.

Table III. Equilibrium Constants for the Reaction *N*-Formyl- + $H^+ \rightleftharpoons$ S + H_2O, $K_{eq} = [S]/[N\text{-formyl}]a_{H^+}$[a]

Substituent	Buffer (pH)	Mole fraction of S at equil	$K_{eq}^{(N\text{-}1)}$	$K_{eq}^{(N\text{-}10)}$
p-CO_2Et	Succinate (5.33)			1.5×10^5
	Succinate (5.76)			1.8×10^5
	Formate (1.87)	0.93	9.2×10^2 [b]	
	Formate (3.14)	0.45	11×10^2	
p-Cl	Succinate (5.41)	0.08	2.3×10^4	
	Formate (4.52)	0.31	1.9×10^4	
p-CH_3	Succinate (5.33)	0.32	1.3×10^5	
	Succinate (5.76)	0.20	1.4×10^5	

[a] With the exception of the H^+ + N^{10}-formyl $\rightleftharpoons$ S + H_2O equilibrium which is discussed in the text, all equilibrium constants were determined from $K_{eq} = OD_\infty/(OD_0 - OD_\infty)(1/a_{H^+})$ at 365 (*p*-CO_2Et) or 355 mμ (*p*-Cl and *p*-CH_3). Equilibria were also approached from the *N*-formyl side under similar conditions and uv scans on the equilibrium mixtures were identical for approach to equilibrium from either side. [b] At this pH, there is less than 1% N^{10}-formyl relative to formamidinium salt.

Product Distribution

The initial partitioning of the *p*-ethoxycarbonylformamidinium salt with respect to the N^1- and N^{10}-formyl products was determined by four different methods depending upon reaction conditions. The methods used were (1) calculation of $k_3/(k_3 + \beta_1)$ as described earlier, (2) calculation of the same from k_3/β_1 using parameters 8 and 10 of Table II, (3) extrapolation of a plot of $[N\text{-}1]/[N]_{total}$ against time to $t = 0$, and (4) where isomerization is slow, measurement of $[N\text{-}1]/[N]_{total}$ spectrophotometrically at 8–10 half-lives for salt hydrolysis. The values thus obtained appear in Table IV. The concentrations of S and N^1- and N^{10}-formyl in any given mixture were determined from the ultraviolet spectrum by use of three simultaneous equations as described in the Experimental Section.

Table IV. Partitioning Values for Kinetic Formation of *p*-CO_2Et Related N^1- and N^{10}-Formyl Compounds

Buffer (*M*)	pH	$[N\text{-}1]/[N_T]$	Method[a]
Phosphate (0.040)	8.15	0.13	4
Phosphate (0.040)	7.33	0.16	3
Phosphate (0.040)	7.11	0.17	3
Phosphate (0.040)	6.76	0.18	3
Phosphate (0.040)	6.15	0.19	3
Succinate (0.054)	6.20	0.17	3
Succinate (0.054)	5.76	0.17	3
Succinate (0.054)	5.76	0.11	2
Succinate (0.054)	5.76	0.15	1
Succinate (0.054)	5.33	0.22	2
Succinate (0.054)	5.33	0.21	1
Tris (0.020)	8.51	0.04	4
Tris (0.020)	8.16	0.04	4
Tris (0.050)	8.16	0.05	4
Tris (0.040)	7.82	0.05	4
H_2O	7.00	0.12	4

[a] 1, from parameters 6 and 8; 2, from parameters 8 and 10 as described in the text; 3, $[N\text{-}1]/[N]_T$ *vs.* time extrapolated to $t = 0$; 4, uv scan at $10t_{1/2}$.

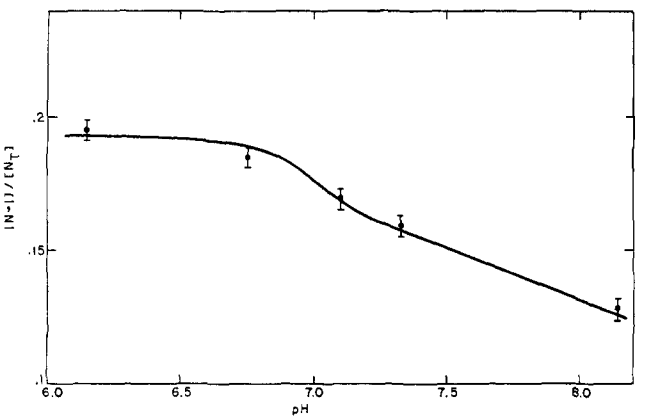

Figure 3. Partitioning values for hydrolysis of the *p*-ethoxycarbonylformamidinium salt (IV) as a function of pH at constant (0.04 *M*) phosphate buffer concentration. Values are from Table IV. The curve is calculated from eq 11.

The partitioning values for hydrolysis of the *p*-ethoxycarbonylformamidinium salt as a function of pH at constant phosphate buffer concentration are presented in Figure 3. The line approximating the points was calculated from eq 11 in which $a = 0.106$, $b = 0.241$,

$$[N^1\text{-formyl}]/[N\text{-formyl}]_{total} = \frac{ak_{H_2O} + bk_B[B] + ck_{B\cdot OH}[B]a_{OH^-}}{k_{obsd}} \quad (11)$$

and $c = 0.124$ represent the mole fraction of N^1-formyl product arising from the k_{H_2O}, $k_B[B]$, and $k_{B\cdot OH}[B]a_{OH^-}$ terms, respectively. Although the total change in mole fraction is only 0.07, the change in relative contribution of each term to k_{obsd} is large and the fit is highly sensitive to small changes in *a*, *b*, and *c*. A reasonable fit could not be obtained when *a*, *b*, or $c = 0$. To corroborate the value for *a*, a separate run was conducted in the absence of buffer with the aid of an autotitrator. The values thus obtained for k_{H_2O} and *a* were in good agreement with those obtained from the experiments conducted in phosphate buffers.

Discussion

The kinetics of hydrolysis of the formamidinium salts IV–VI as expressed in eq 1 are qualitatively similar to those describing the base-catalyzed hydrolysis of 1,3-diphenyl-2-imidazolinium chloride reported by Robinson and Jencks.[4] Moreover, the arguments advanced by those authors in development of their proposed mechanisms are presumably applicable to the reactions reported here. In an accompanying paper, Robinson and Jencks reported the results of similar reactions involving 5,10-methenyltetrahydrofolic acid and proposed mechanisms analogous to those of the model compound.[6] The mechanisms proposed (eq 12 and 13) involve preequilibrium addition of OH^- to the formamidinium salt followed by rate-limiting general acid catalyzed decomposition of the anionic tetrahedral addition compound (eq 13) or by general base catalyzed breakdown of the cationic intermediate (eq 12). That the second step is rate determining at pH >3—which encompasses our kinetics—was checked by monitoring the reverse reaction from either N^1-formyl or N^{10}-formyl to IV at pH 2 and 3.2, respectively. The value of k_{H_2O} calculated from these data and the equilibrium constants agreed with k_{H_2O} determined for hydrolysis of IV above pH 6. Several lines of evidence for the intermediacy of a tetrahedral addition compound in amidine hydrolysis have been reported, including its direct spectrophotometric observation under strongly alkaline conditions where the rate of breakdown is depressed due to an unfavorable ionization of the intermediate.[7] Mechanisms 12 and 13 then are apparently consistent with all of the data thus far reported, with the possible exception of formation of the N^1-formyl derivative of I, the mechanism for which will be described in a separate communication. It is interesting to note that the mechanisms of eq 12 and 13 predict that, in the absence of other effects, the orientation of breakdown of the tetrahedral intermediate would be a reflection of the relative microscopic pK_a values of N-1 and N-10—pK_a (N-1, I–III) 4.35; pK_a (N-10, I) 2.23; pK_a (N-10, II) 3.98; pK_a (N-10, III) 5.12—estimated from the pK_a values of the parent anilines.[9] Formation of the N^{10}-formyl isomer is observed, however, only in hydrolysis of IV for which $\Delta pK_a \cong 2$. Hydrolysis of V for which the basicities of N-1 and N-10 are comparable gives none of the N^{10}-formyl isomer indicating the geometry to be important in partitioning of the intermediate.

The interpretation of the linear dependence on pK_a of K_{eq}^{N-1} is not straightforward. Although intuitively one might argue that the positively charged methenyl carbon of the formamidinium salt is subject to inductive and resonance effects which are proportional to the respective aniline–anilinium H^+ equilibria, the effect of pK_a on the stability of the N^1-formyl derivatives must also be included. Unfortunately these effects presently may not be separated.

The inherent symmetry of 1,3-diphenyl-2-imidazolinium chloride allows formation of only one monoformylated hydrolysis product and thereby avoids the questions of mixed formyl products and/or product isomerization. Although 5,10-methenyltetrahydrofolic

acid is dissymmetric, Robinson and Jencks reported that under hydrolytic conditions at pH >6, N^{10}-formyltetrahydrofolic acid is formed exclusively.[6] In contrast to this, the dissymmetric model formamidinium salt IV yields a mixture of the N^1- and N^{10}-formyl hydrolysis products under conditions of kinetic control where the mole fraction of N^1-formyl varies from ~0 to ~20% depending on the nature of the buffer species present. The latter represents a difference of <1 kcal for the respective product-determining steps. Since the pathway for production of N^1-formyl compound is only slightly higher energetically than that for formation of the N^{10}-formyl and the equilibrium of eq 10 favors the N^1-formyl product it is reasonable that isomerization should occur whenever the I → N^{10}-formyl step becomes reversible. As indicated in the results, this is observed.

The kinetic data obtained for hydrolysis of the *p*-ethoxycarbonylformamidinium salt (IV) under conditions where isomerization is kinetically significant can be rationalized in terms of at least two schemes (I and II). Both schemes allow for the experimentally ob-

Scheme II

$$N^{10}\text{-formyl} \rightleftharpoons I' \rightleftharpoons S \rightleftharpoons I'' \longrightarrow N^1\text{-formyl}$$

served equilibrium established between the salt IV and N^{10}-formyl compound prior to the slower, irreversible production of N^1-formyl. Assuming that I′ and I″ are steady-state intermediates on the reaction pathway, then Scheme II simplifies to N-10 ⇌ S → N-1 for which the parametric equations are known.[8] This scheme does not predict the lag phase in the production of N^1-formyl from formamidinium salt as is observed (figure not shown). A data-allowed permutation of Scheme II, *i.e.* S ⇌ N-10 → N-1, similarly fails to generate a lag phase in the formation of N-1 from N-10 as is observed (Figure 1). Only the symmetrical Scheme I appears to possess the necessary characteristics to generate lag phases for the formation of the N^1-formyl derivative from both the formamidinium salt IV and for the N^{10}-formyl compound.

As indicated in Table IV, the ratio of the N^1- and N^{10}-formyl products obtained upon hydrolysis of the *p*-ethoxycarbonylformamidinium salt above pH 6—under kinetic control—varies with reaction conditions. Analysis of the data revealed that the product composition is a function of catalyst type and is not a function of pH except insofar as the concentrations of the acid and base forms of the buffer catalysts are pH dependent. For example, phosphate buffer held at a pH typical of the Tris runs (8.16) by an autotitrator generated a product mixture containing 13% N^1-formyl whereas Tris alone results in *ca.* 5% N^1-formyl production.

Since mechanisms 12 and 13 are well supported and ring opening is by definition the product- and rate-determining step, the product composition must be related in a simple fashion to the kinetic terms contributing to k_{obsd}. This assumption is the basis for eq 11 and the related figure. Although separation of kinetic terms and evaluation of partitioning constants were performed for the phosphate-catalyzed reactions only, a number of indicative results can be seen in the product distribution of reactions conducted in other buffers. From the catalytic constants of Table I and the observed product distributions of Table IV, one may estimate the *b* term (eq 11) for the phosphate, succinate, and Tris buffers. The order is succinate > phosphate > Tris.

Making no attempt to advance a quantitative argument, one can rationalize these data with the simple hypothesis that the catalytic constants for production of the two *N*-formyl compounds in hydrolysis of IV both might follow the Brønsted relationship but each with a different Brønsted coefficient. For any one kinetic term then, the product ratio is a function of the catalyst's pK_a and the ratio of the respective Brønsted coefficients.

The kinetic and thermodynamic dispositions of the *p*-ethoxycarbonylformamidinium salt and the related *N*-formyl derivatives are qualitatively and in some respects quantitatively analogous to those of the corresponding derivatives of tetrahydrofolic acid. By way of comparison, the work of Shive, *et al.*,[4] describes the nonenzymic interconversion of formate-carrying FH_4 derivatives. To recapitulate: (1) hydrolysis of 5,10-methenyltetrahydrofolic acid under basic conditions yields mostly N^{10}-formyltetrahydrofolic acid with small amounts of N^5-formyl arising concomitantly; (2) acidification of either the N^5- or N^{10}-formyl derivatives effects reconversion to the starting salt; (3) under certain conditions, *e.g.*, autoclaving or prolonged incubation in weakly basic medium, an aqueous solution of N^{10}-formyltetrahydrofolic acid undergoes slow isomerization to N^5-formyltetrahydrofolic acid. As mentioned earlier, hydrolysis of 5,10-methenyltetrahydrofolic acid exhibits the same kinetics as the model compound IV with the exception that the former suffers a rate depression attributed to ionization of the amide function in the pyrimidine ring.

Lastly, the equilibrium constants relating the model formyl compounds to the formamidinium salt and thereby also to one another are essentially in quantitative agreement with those of the natural cofactor[10] indicating the ground-state energies to be about the same and apparently independent of the remote functionality of the natural cofactor.

The only mechanistic study of the nonenzymic reactions of formate-carrying tetrahydrofolic acid is that of Robinson and Jencks. The extent to which the *p*-CO_2Et model compounds mimic the natural cofactors, however, suggests that the kinetics and implied mechanisms of the reactions reported here might closely resemble the analogous reactions of FH_4. In view of this, these and other reactions of the model are currently under further investigation.

The biochemical implications of the work reported here are straightforward, but advanced with some trepidation, keeping in mind that this is an investigation of nonenzymic reactions of model compounds. First, the ability of the N^{10}-formyl model to isomerize to N^1-formyl, albeit quite slowly with most catalysts, might afford some rationale for the fact that N^5-formyltetrahydrofolic acid is found in significant levels in

(10) L. D. Kay, M. J. Osborn, Y. Hatefi, and F. M. Huennekens, *J. Biol. Chem.*, **235**, 195 (1960). The equilibrium constants interrelating N^5,N^{10}-methenyl-, N^5-formyl-, and N^{10}-formyltetrahydrofolic acid are: $K_1 = [N^5,N^{10}\text{-CH}{\equiv}FH_4]/[N^{10}\text{-HCOF}H_4]a_{H^+} = 0.9 \times 10^6\ M^{-1}$; $K_2 = [N^5,N^{10}\text{-CH}{\equiv}FH_4]/[N^5\text{-HCOF}H_4]a_{H^+} = 6.5 \times 10^2\ M^{-1}$; $K_3 = [N^5\text{-HCOF}H_4]/[N^{10}\text{-HCOF}H_4] = 1.4 \times 10^3$. The value for K_2 is questionable since equilibrium could apparently be approached only from the N^5-formyltetrahydrofolic acid side.

some cells, but a protein possessing N^5-formyltetrahydrofolic acid synthetase activity has not been isolated.[3] Secondly, in spite of the fact that 5,10-methenyltetrahydrofolic acid can hydrolyze directly to N^5-formyltetrahydrofolic acid, a subtle energy barrier directs even nonenzymic hydrolysis toward the less stable but biologically useful N^{10}-formyltetrahydrofolic acid. Any metabolic excess of the latter might then relax to its more stable isomer. Finally, almost trivially, it would seem that interconversion of the three formate-carrying cofactors discussed here, with the probable exception of the ATP-dependent N-5,N-10 transformylation, could involve relatively simple enzymic mechanisms employing only well-positioned proton acceptor and donor groups.

At a minimum, these data further support the hypothesis upon which design of the model was predicated, that the central features of FH_4 chemistry are highly dependent on the ΔpK_a between N-5 and N-10 and essentially independent of the pyrimidine moiety and glutamate residue(s), those functioning principally in binding of the cofactor to the appropriate protein surfaces.

Experimental Section

Materials. Synthesis of ethyl *p*-[*N*-2′-(1,2,3,4)-tetrahydroquinoxalinylmethylene]aminobenzoate and the related CH_3 and Cl derivatives (I, II, and III) has been previously described.[5,11]

The corresponding formamidinium compounds were prepared as the fluoroborate salts as follows. Compound I (150 mg, ~0.5 mmol) was dissolved in 15 ml of ethanol and triethyl orthoformate (0.1 ml, 0.6 mmol) was added with stirring at room temperature. After ~5 min 1 ml of fluoroboric acid (50% aqueous solution, Baker and Adamson) was added dropwise. The formamidinium salt crystallized immediately as bright yellow fine needles. The precipitate was filtered and dried *in vacuo*. Recrystallization from methanol acidified with fluoroboric acid did not alter the melting point.

***p*-Ethoxycarbonylformamidinium fluoroborate** (IV) showed a yield of >90%, mp 260–265°. The ultraviolet spectrum exhibited $\lambda_{max}^{pH\ 3}$ 363 (ε 13,700) and 308 mμ (ε 15,500). The nmr spectra of the three formamidinium fluoroborate salts IV, V, and VI were poorly defined due to their limited solubility in suitable solvents, but all exhibited an absorption integrating to *ca.* one proton δ ~10 (relative to TMS) corresponding to the methenyl proton.

Anal. Calcd for $C_{19}H_{20}N_3O_2BF_4$: C, 55.75; H, 4.89; N, 10.26. Found: C, 55.71; H, 5.46; N, 10.22.

***p*-Chloroformamidinium fluoroborate** (V) showed a yield of >90%, mp 290–294°. The uv spectrum exhibited $\lambda_{max}^{pH\ 4.5}$ 354 (ε 13,200) and 304 mμ (ε 12,600).

Anal. Calcd for $C_{16}H_{15}N_3ClBF_4$: C, 51.71; H, 4.04; N, 11.31. Found: C, 51.50; H, 3.75; N, 11.02.

***p*-Methylformamidinium fluoroborate** (VI) showed a yield of 70%, mp 274–277°. The uv spectrum exhibited $\lambda_{max}^{pH\ 3}$ 351 (ε 13,400) and 303 mμ (ε 11,600).

Anal. Calcd for $C_{17}H_{18}N_3BF_4$: C, 58.12; H, 5.13; N, 11.97. Found: C, 57.45; H, 5.60; N, 11.67.

Formyl Derivatives. With the exception of the N^1-formyl hydrollysis product from the *p*-ethoxycarbonylformamidinium fluoroborate salt, the *N*-formyl derivatives of I, II, and III were prepared as follows.

The formamidinium salt (150 mg, ~0.5 mmol) was added to 150 ml of 2 *M* K_2HPO_4 containing 100 ml of ether and the heterogeneous mixture was stirred vigorously until clear and free of yellow color. The ether phase was separated and the aqueous phase extracted with ether (100 ml). The combined ether extracts were dried over potassium carbonate and stripped of solvent on a rotary evaporator. The residual solid was recrystallized from ethanol–water.

Preparation of the N^1-formyl derivative of IV was as follows. The N^{10}-formyl derivative of IV (30 mg, 0.1 mmol) was added to a solution of ethanol (25 ml) and aqueous succinate buffer (25 ml, 0.067 *M*, pH 5.33). The mixture was stirred for 24 hr at room temperature and then extracted with ether (three 30-ml portions). The combined ether extracts were dried over potassium carbonate and freed of solvent. The residual solid was recrystallized from ethanol–water. The uv spectra of the isolated *N*-formyl compounds are identical with those observed in kinetic runs.

The N^1-formyl derivative of I showed a yield of >90%, mp 161–162°, needles. The uv spectrum exhibited $\lambda_{max}^{H_2O}$ 307 mμ (ε 25,700). The nmr spectrum in Silanor C exhibited, among other absorptions, the following: δ 1.45 (t, 3, J = 7 Hz, CH_3), 4.4 (q, 2, J = 7 Hz, CH_2), 6.8 (m, 6, aromatic H of quinoxaline moiety and meta H of *p*-aminobenzoate moiety), 7.9 (d, 2, ortho H of *p*-aminobenzoate moiety part of an AA′XX quartet, J_{AX} = 9 Hz), 8.9 (s, 1, HC=O). The mass spectrum gave as molecular ion a peak at *m/e* 339.

Anal. Calcd for $C_{19}H_{21}N_3O_3$: C, 67.26; H, 6.19; N, 12.39. Found: C, 66.66; H, 5.79; N, 12.04.

The N^{10}-formyl derivative of I showed a yield of >90%, mp 108–110°, needles. The uv spectrum exhibited $\lambda_{max}^{H_2O}$ 255 mμ (ε 14,700). The nmr spectrum in Silanor C exhibited among others the following absorptions: δ 1.45 (t, 3, J = 7 Hz, CH_3), 4.4 (q, 2, J = 7 Hz, CH_2), 7.32 and 8.18 (q, 2 each, AA′XX′ system of ethyl *p*-aminobenzoate moiety, J_{AX} = 8.5 Hz), 6.6 (s, 4, aromatic H of quinoxaline moiety), 8.65 (s, 1, HC=O). The mass spectrum gave a molecular ion peak at *m/e* 339.

Anal. Calcd for $C_{19}H_{21}N_3O_3$: C, 67.26; H, 6.19; N, 12.39. Found: C, 67.31; H, 6.15; N, 12.54.

The N^1-formyl derivative of II showed a yield of >90%, mp 167–170°, needles. The uv spectrum exhibited $\lambda_{max}^{H_2O}$ 307 mμ (ε 3800). The nmr spectrum exhibited among others the following absorptions: δ 6.8 (br m, 8, aromatic H), 8.9 (s, 1, HC=O). The mass spectrum gave the molecular ion peak at *m/e* 301.

Anal. Calcd for $C_{16}H_{16}N_3OCl$: C, 63.68; H, 5.31; N, 13.93. Found: C, 63.10; H, 5.36; N, 13.81.

The N^1-formyl derivative of III showed a yield of >90%, mp 153–155°, needles. The uv spectrum exhibited $\lambda_{max}^{H_2O}$ 308 mμ (ε 5500). The nmr spectrum exhibited among others the following absorptions: δ 2.2 (s, 3, $ArCH_3$), 6.75 (m, 8, aromatic H), 8.75 (s, 1, HC=O). The mass spectrum gave a molecular ion peak at *m/e* 281.

Anal. Calcd for $C_{17}H_{16}N_3O$: C, 72.60; H, 6.76; N, 14.95. Found: C, 72.70; H, 6.63; N, 14.99.

Reduction of IV. Sodium borohydride (10 mg, ~0.25 mmol) was added to a stirred solution of IV (20 mg, ~0.05 mmol) in THF (20 ml). When the reaction mixture was free of yellow color, water was added (5 ml) and the resultant mixture was extracted with benzene (two 10-ml portions). Solvent was removed from the extract leaving a crystalline solid which was recrystallized from benzene–hexane: yield >90%, mp 168–169° (lit. 168–169°).[5]

Kinetics. The instruments employed have been previously described.[12] All reagents used were reagent grade.

Kinetic runs (25°) were initiated by addition of 0.02 ml of a stock solution of the desired tetrahydroquinoxaline derivative to a cuvette containing 2 ml of aqueous buffer. The final reactant concentration was 5×10^{-5} *M*, μ = 0.2, KCl. The stock solutions were freshly prepared with either spectral grade methanol (*N*-formyl compounds) or dried DMF (formamidinium salts), the latter giving no appreciable absorption above 250 mμ. The course of the reactions involving formamidinium salt hydrolysis was monitored by observing OD decrease at 365 (*p*-CO_2Et) or 350 mμ (*p*-Cl, *p*-CH_3) corresponding to disappearance of reactant. Where rates were pseudo first order, k_{obsd} (±5%) was taken as slope × 2.303 from a plot of log ($OD_t - OD_\infty$) *vs.* time. Product distributions were determined from ultraviolet spectra run at 8–10 half-lives by the method described below. The pH of reaction solutions taken before and after runs agreed within 0.02 unit. Values for a_{OH^-} were taken as $10^{-14}/a_{H^+}$.

Where the kinetics deviated from first order, the concentrations of the three *p*-ethoxycarbonyltetrahydroquinoxaline derivatives (N^1-formyl, N^{10}-formyl, and formamidinium salt) were followed by obtaining sequential ultraviolet scans (Cary 14) on the progressing reaction and applying three simultaneous equations involving OD's at three wavelengths. The solved equations were $[N^1\text{-formyl}] = 0.509A_{300} - 0.137A_{260} - 0.443A_{365}$, $[N^{10}\text{-formyl}] = 0.687A_{260} - 0.295A_{300} - 0.105A_{365}$, and $[S] = 0.73A_{365}$, where A_{300}, A_{260}, and A_{365} are observed OD values at 300, 260, and 365 mμ, respectively. Under conditions where change in optical density at a given wave-

(11) S. J. Benkovic, P. A. Benkovic, and R. L. Chrzanowski, *J. Amer. Chem. Soc.*, 93, 523 (1970).

(12) S. J. Benkovic and P. A. Benkovic, *ibid.*, 88, 5504 (1966).

length was significant over the time required for a scan, OD values were determined by interpolation on a plot of OD_λ *vs.* time. The extinction coefficients used to set the simultaneous equations

Compd (derived from I)	$\epsilon_{365} \times 10^{-4}$	$\epsilon_{300} \times 10^{-4}$	$\epsilon_{260} \times 10^{-4}$
S	1.37	1.41	0.812
N^1-Formyl	0	2.22	0.935
N^{10}-Formyl	0	0.44	1.64

were pH invariant in the range of investigation. In the course of a given reaction, the total molar concentration as calculated above varied by less than 1% up to 90% of reaction.

The computer program used for least-squares fitting is described elsewhere.[13]

The values for buffer pK_a values were taken as the pH of the half-neutralized buffer solution.

Acknowledgment. We are grateful to the National Science Foundation (GB 16789) for support of this investigation.

(13) S. J. Benkovic and E. Miller, *Bioinorg. Chem.*, 1, 107 (1972).

Nuclear Magnetic Resonance Studies of the Interaction of *N*-Formyltryptophanate with α-Chymotrypsin

J. T. Gerig* and R. A. Rimerman[1]

Contribution from the Department of Chemistry, University of California, Santa Barbara, California 93106. *Received May 25, 1971*

Abstract: High-resolution proton magnetic resonance techniques have been used to study the interaction of *N*-formyl-L-tryptophanate with the proteolytic enzyme α-chymotrypsin and with the catalytically inactive tosyl derivative of this protein at apparent pH 6.2 in deuterium oxide solution. In the presence of the enzyme, marked upfield chemical shifts are observed for the aromatic protons of this inhibitor, as well as with the corresponding D isomer. These shifts are tentatively interpreted in terms of interactions between the tyrosine-228 side chain at the active site of the protein and the inhibitor molecule. Consideration of protein-induced line-broadening effects indicates that both forms of the inhibitor bind tightly to the enzyme while the chemical-shift effects are consistent with the conclusion that the inhibitor–enzyme complex has essentially the same structure in aqueous solution that has been determined for the crystalline form.

Although chemical studies with enzyme model systems can often provide considerable insight into the mechanisms of enzyme catalysis,[2] there is no substitute for the understanding that accurate information about the three-dimensional structure of the enzyme provides. The development of X-ray crystallographic methods for the determination of protein structures has been an all-important step in this regard and, despite sometimes formidable experimental problems, the crystal structures of a number of enzymes have been determined by this method.[3,4] However, the correspondence between the structure of the protein in the crystalline environment and its form in aqueous solution under physiological conditions must be established by additional chemical and spectroscopic experimentation.

Blow and his coworkers have described X-ray crystallographic studies of tosyl-α-chymotrypsin[5] and have also examined the structures of several complexes of chymotrypsin with inhibitors, including *N*-formyl-L-tryptophan.[6] Nuclear magnetic resonance experiments have provided useful information about enzyme–inhibitor complexes in solution for several systems[7] and, in view of the wide interest in α-chymotrypsin and the availability of the above-mentioned crystallographic results, we decided to examine the solution-state complex formed between this enzyme and *N*-formyltryptophan by these high-resolution nmr techniques. The results of this investigation are described below.

Results

The spectrum of this inhibitor as a 51 m*M* solution in D_2O (apparent pH 6.2) obtained at 100 MHz is shown in Figures 1 and 2. The spectrum is similar to that found for tryptophan,[8] with an ABCD pattern for the aromatic protons (H_1–H_4) and a broad singlet for the vinyl proton (H_V) appearing at low field and the

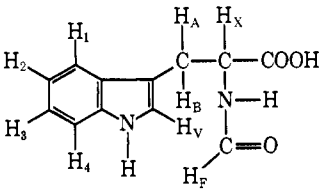

AB part of two sets of ABX signals apparent at higher fields. It is clear from Figure 2 that two different ABX systems are present in the spectrum, probably due to

(1) U. S. Public Health Service Predoctoral Fellow, 1968–1971. This work will form a portion of the Ph.D. Thesis of R. A. R. A preliminary report has appeared: *Biochem. Biophys. Res. Commun.*, 40, 1149 (1970).
(2) T. C. Bruice and S. J. Benkovic, "Bioorganic Mechanisms," W. A. Benjamin, New York, N. Y., 1966.
(3) See *Phil. Trans. Roy. Soc. London, Ser. B*, 257, 65 (1970).
(4) D. Eisenberg, "The Enzymes," 3rd ed, P. D. Boyer, H. Lardy, and K. Myrbaeck, Ed., Vol. 1, Academic Press, New York, N. Y., 1970, p 1.
(5) (a) P. B. Sigler, D.M. Blow, B. W. Matthews, and R. Henderson, *J. Mol. Biol.*, 35, 143 (1968); (b) R. Henderson, *ibid.*, 54, 341 (1970).
(6) T. A. Steitz, R. Henderson, and D. M. Blow, *ibid.*, 46, 337 (1969).
(7) (a) G. C. K. Roberts and O. Jardetzky, *Advan. Protein Chem.*, 24, 447 (1970); (b) M. A. Raftery and F. W. Dahlquist, *Fortschr. Chem. Org. Naturst.*, 27, 341 (1969).
(8) J. T. Gerig, *J. Amer. Chem. Soc.*, 90, 2681 (1968).